

Optimal synchronization of circulant and non-circulant oscillators

Shirin Panahi^a, Fahimeh Nazarimehr^a, Sajad Jafari^{a,b}, Julien C. Sprott^c,
Matjaž Perc^{d,e,f,*}, Robert Repnik^d

^a Biomedical Engineering Department, Amirkabir University of Technology, Tehran, Iran

^b Health Technology Research Institute, Amirkabir University of Technology, Tehran, Iran

^c Department of Physics, University of Wisconsin - Madison, Madison, WI 53706, U.S.A.

^d Faculty of Natural Sciences and Mathematics, University of Maribor, Koroška cesta 160, Maribor 2000, Slovenia

^e Department of Medical Research, China Medical University Hospital, China Medical University, Taichung, Taiwan

^f Complexity Science Hub Vienna, Josefstädterstraße 39, Vienna 1080, Austria

ARTICLE INFO

Article history:

Received 5 October 2020

Revised 15 November 2020

Accepted 22 November 2020

Keywords:

Circulant oscillator

Non-circulant oscillator

Single variable coupling

Multi-variable coupling

Master stability function

ABSTRACT

We study the synchronization of coupled identical circulant and non-circulant oscillators using single variable and different multi-variable coupling schemes. We use the master stability function to determine conditions for synchronization, in particular the necessary coupling parameter that ensures a stable synchronization manifold. We show that for circulant oscillators, the smallest coupling parameter for synchronization is needed when multi-variable coupling with the same coupling coefficients is applied. Conversely, for non-circulant oscillators, no such general conclusions are attainable in that the smallest coupling parameter cannot be attributed to a particular coupling setup.

© 2020 Elsevier Inc. All rights reserved.

1. Introduction

Chaos is a challenging behavior in dynamical systems [1,2]. Many studies aim to understand the generation process of chaotic dynamics and investigate the properties of chaotic flows. Chaotic dynamics are studied in different fields of science. For example, emergence of chimera states in a chaotic neural network was discussed in [3]. FPGA realization of a chaotic system was studied in [4]. In [5], fractional-order chaotic dynamics were discussed. A fractional-order memristive chaotic circuit was investigated in [6]. Control of chaotic systems is essential [7]. The sliding mode control of a fractional-order chaotic system is also studied in [8].

Dynamical networks and their properties are vital in the study of complex dynamics [9,10]. The study of epidemic spread and its vaccination is one such examples [11]. Also, it can be used to study the nonlinear interactions between the dynamical process of climate events [12]. Investigating the dynamical properties of the brain as a neural network can be considered as another application of dynamical networks [13]. Synchronization is one of the most important behaviors in complex dynamical networks [14]. Investigating the dynamical network's synchronization can be more challenging if the dynamics of the oscillators in each node of the network are chaotic. Many studies have been done on the subject of synchronization of the dynamical networks [15–17]. This phenomenon is considered as an appropriate tool in the study of dynamical networks

* Corresponding author at: Faculty of Natural Sciences and Mathematics, University of Maribor, Koroška cesta 160, 2000 Maribor, Slovenia.
E-mail address: matjaz.perc@um.si (M. Perc).

[18]. Synchronization can be affected by different factors of dynamical networks such as coupling parameters, the dynamical oscillator in each node, and the topology of the networks. For example, the effect of different coupling structures (such as coupling through various variables) on the synchronization is analyzed in dynamical networks with the same topology [19]. Field coupling synchronization was studied in memristive chaotic systems in [20]. Furthermore, the synchronization of a network with fractional-order systems in each node has been investigated [21]. The emergence of synchronized dynamics in coupled Rössler oscillators was discussed in [22]. Also, the synchronization of neural networks has received much attention from the biological perspective [23]. The effect of the electromagnetic field on the synchronization of the Hindmarsh-Rose neural network was studied in [24].

The first step in investigating the synchronizability of the network is to find the proper conditions for the incidence of the stable synchronization manifold. Most of the research in the literature tries to understand the fundamental interaction between network topology and synchronization. For example, in 1996, Wu and Chua advanced a conjecture, which can be considered as an important milestone in this field of research [25]. They claimed that the proper coupling parameter for synchronization can be scaled by the second largest eigenvalue of the connectivity matrix. However, two years later, Pecora and Carroll revealed that this conjecture is not always true. Instead, they proposed a new approach called Master Stability Function (MSF), which investigates the necessary condition of the local synchronization for identical networks [26]. After that, the MSF method was developed for a complex network with time-varying coupling [27] and multi-layer networks [28] or even for non-identical networks [29].

There are different types of coupling structures that can be added to each variable of the coupled oscillators. To emphasize and investigate just the effect of the coupling structure on the network's synchronizability, authors in [19] have suggested that it is better to use two coupled circulant oscillators. Circulant oscillators have been used in some references [30,31]. Circulant refers to a dynamical system with cyclically symmetric states but with the same functional form [32]. For example, a circulant oscillator can be formulated as:

$$\begin{aligned}\dot{x} &= f(x, y, z) \\ \dot{y} &= f(y, z, x) \\ \dot{z} &= f(z, x, y)\end{aligned}\quad (1)$$

The results showed that multi-variable coupling has better synchronizability than single-variable coupling. In this paper, some multi-variable couplings with different coupling coefficients are compared with previous cases to find the best coupling cases for synchronization. Also, the results of circulant and non-circulant oscillators are compared.

2. Proposed method

It has been shown that identical networks with a specific oscillator in each node share the different zero-crossing points in the MSF diagram when the coupling is applied to different variables (states) [33]. In this study, a different way of dividing the coupling parameter among various links and states, which affects the synchronization, is investigated. For the sake of simplicity, in each case, we consider a network consisting of only a pair of oscillators. Various couplings are defined as follows,

$$\begin{aligned}\dot{x}_1 &= f_1(x_1, y_1, z_1) + d\alpha_1(x_2 - x_1) & \dot{x}_2 &= f_1(x_2, y_2, z_2) + d\alpha_1(x_1 - x_2) \\ \dot{y}_1 &= f_2(x_1, y_1, z_1) + d\alpha_2(y_2 - y_1) & \dot{y}_2 &= f_2(x_2, y_2, z_2) + d\alpha_2(y_1 - y_2) \\ \dot{z}_1 &= f_3(x_1, y_1, z_1) + d\alpha_3(z_2 - z_1) & \dot{z}_2 &= f_3(x_2, y_2, z_2) + d\alpha_3(z_1 - z_2)\end{aligned}\quad (2)$$

where the α_i coefficients affect the strength of the coupling in the various cases. To keep the sum of all coupling parameters equal to d , the following condition is assumed:

$$\alpha_1 + \alpha_2 + \alpha_3 = 1. \quad (3)$$

Thus the coupling vector is

$$\text{Vec}_d = (d\alpha_1, d\alpha_2, d\alpha_3)^T \quad (4)$$

In this study, seven coupled oscillators consisting of seven different oscillators are studied to investigate the effect of coupling on various variables. The first four coupled oscillators consist of circulant oscillators, and the others consist of non-circulant oscillators. In circulant oscillators, all the states have the same dynamical properties. The studied oscillators are discussed in the following.

1) Piecewise linear: This oscillator has a chaotic solution for initial conditions $(x_0, y_0, z_0) = (0.4, 0, 0)$.

$$\begin{aligned}\dot{x} &= 1 - x - y - 4|y| \\ \dot{y} &= 1 - y - z - 4|z| \\ \dot{z} &= 1 - z - x - 4|x|\end{aligned}\quad (5)$$

2) Cubic: This oscillator has a chaotic attractor for initial conditions $(x_0, y_0, z_0) = (-0.77, 0.35, 1.13)$.

$$\begin{aligned}\dot{x} &= y^3 - z \\ \dot{y} &= z^3 - x \\ \dot{z} &= x^3 - y\end{aligned}\quad (6)$$

Circulant oscillator: Cubic

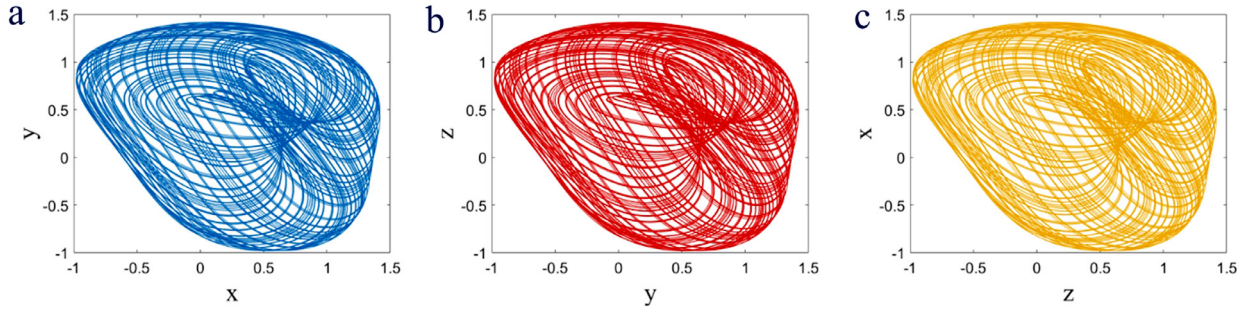


Fig. 1. The different projection of state space for a circulant system. Circulant oscillators show symmetric state space.

Non-circulant oscillator: Rössler

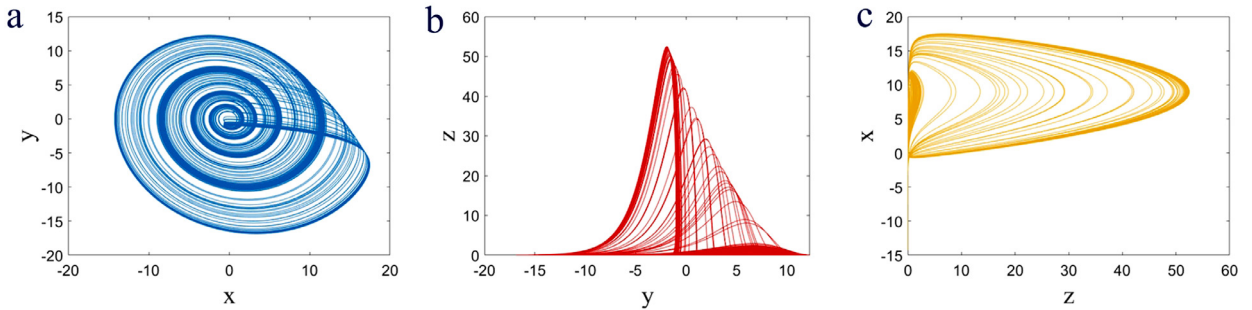


Fig. 2. The different projection of state space for a non-circulant system. Non-circulant oscillators show asymmetric state space.

3) Quadratic: For initial conditions $(x_0, y_0, z_0) = (0.7, 0.6, 1.2)$ this oscillator has a chaotic attractor.

$$\begin{aligned} \dot{x} &= y^2 - z \\ \dot{y} &= z^2 - x \\ \dot{z} &= x^2 - y \end{aligned} \tag{7}$$

4) Thomas: This oscillator has a chaotic attractor for $(x_0, y_0, z_0) = (0.4, 0, 0)$.

$$\begin{aligned} \dot{x} &= -x + 4y - y^3 \\ \dot{y} &= -y + 4z - z^3 \\ \dot{z} &= -z + 4x - x^3 \end{aligned} \tag{8}$$

5) Lorenz: This oscillator is investigated with random initial conditions for the parameters $s = 10, r = 28, b = 2$.

$$\begin{aligned} \dot{x} &= s(y - x) \\ \dot{y} &= x(r - z) - y \\ \dot{z} &= xy - bz \end{aligned} \tag{9}$$

6) Rössler: This oscillator is studied for the parameters $a = 0.2, b = 0, c = 4$ and random initial conditions.

$$\begin{aligned} \dot{x} &= -y - z \\ \dot{y} &= x + ay \\ \dot{z} &= b + z(x - c) \end{aligned} \tag{10}$$

7) Hindmarsh-Rose neuron (HR): This oscillator is investigated for $I = 3.2, r = 0.006, s = 4$, and random initial conditions.

$$\begin{aligned} \dot{x} &= y + 3x^2 - x^3 - z + I \\ \dot{y} &= 1 - 5x^2 - y \\ \dot{z} &= -rz + rs(x + 1.6) \end{aligned} \tag{11}$$

Circulant systems have a special form in which the variables are cyclically symmetric. The different projections in state space help to show the difference between the circulant and non-circulant oscillators graphically (Figs. 1 and 2).

For each coupled oscillator, several cases are defined to study the effect of the structure of couplings on the synchronization of the coupled oscillators. In other words, we want to find the best distribution of couplings to have the synchronization

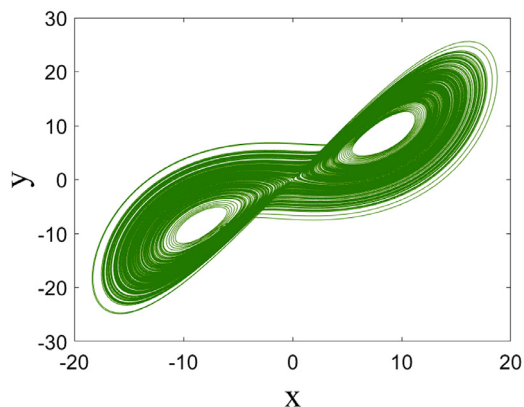


Fig. 3. The chaotic synchronization manifold of identical network consist of Lorenz oscillators ($\mathbf{s}(t)$).

manifold with the smallest coupling parameter d . To find the optimum coupling parameter, which makes the two coupled oscillators synchronized, the MSF approach is used.

The MSF approach checks the synchronizability of identical networks, which consist of diffusely coupled dynamical oscillators [26]. At first, undirected and unweighted identical networks with N individual oscillators are considered as follows:

$$\dot{\mathbf{x}}_i = F(\mathbf{x}_i) - \epsilon \sum_{j=1}^N g_{ij} H(\mathbf{x}_j) \tag{12}$$

where \mathbf{x}_i and $F(\cdot)$ show the variable vector and dynamics of each oscillator, respectively. The parameter ϵ is a coupling parameter, and the Laplacian matrix of $G = [g_{ij}]_{N \times N}$ reveals the topological connection matrix of the network. The projection matrix H determines the coupling types of the network. The $\mathbf{s}(t)$ is the synchronization manifold of the network, which can be defined as:

$$\dot{\mathbf{s}}(t) = F(\mathbf{s}(t)) \tag{13}$$

where $\mathbf{s}(t) = \mathbf{x}_1(t) = \mathbf{x}_2(t) = \dots = \mathbf{x}_N(t)$. For example, the synchronization manifold of the dynamical network consisting of Lorenz oscillators is represented in Fig. 3. To investigate the stability of the synchronization manifold $\mathbf{s}(t)$ of this network, the stability of the block diagonalized variational equation of the network is analyzed,

$$\dot{\eta}_i = DF(s)\eta_i - \epsilon \lambda_i DH(s)\eta_i \quad i = 1, \dots, N \tag{14}$$

where DF and DH are the Jacobian matrixes, and λ_i s are the eigenvalues of the connection matrix G , which are ordered as $\lambda_1 = 0 < \lambda_2 \leq \dots \leq \lambda_N$. To unify the notation of the whole paper, $d_i = \epsilon \lambda_i$ is used as a new notation of the coupling parameter in the rest of the paper. MSF is the largest Lyapunov exponent of Eq. (12). The network can be synchronized in the negative range of the MSF, and the zero-crossings of the MSF diagram can be considered as the minimum value of the coupling parameter of the network required for synchronization.

The previous study of circulant oscillators has shown that the multi-variable case with equal coupling coefficients has the minimum coupling parameter for zero crossings of the MSF compared to the cases with the coupling parameter for each variable separately [19]. In this study, we divide our interests into two groups. In the first group, single variable couplings and various multi-variable couplings with different coupling coefficients are used, and the results are investigated for the circulant oscillators. In the second group, non-circulant oscillators are studied to show the effect of the type of coupling on the synchronization of the two coupled oscillators.

3. Results

In each coupled oscillator, we define some coupling cases with various α_i s, which can test the strength of various couplings in the synchronization. The results of various coupled oscillators are discussed in the following.

In all the coupled circulant oscillators, five cases are used, which are shown in Table 1. The first case is coupling of the x variable. The others are coupling on x, y, z variables unequally, and equally, respectively. For example, Fig. 4 shows the MSF of various cases for the piecewise linear oscillator. The minimum coupling parameter for full synchronization is found in each case. The results in Table 2 show that in all cases, the smallest zero crossings of the MSF function is in case 5 in which all variables are coupled equally with the same coupling coefficient of 0.3333. In the following, the results are just summarized in the tables.

Now the question is what happens if non-circulant oscillators are tested. For that, three coupled oscillators consisting of Lorenz, Rössler, and Hindmarsh-Rose neuron oscillators, were tested. In each of these three coupled oscillators, some

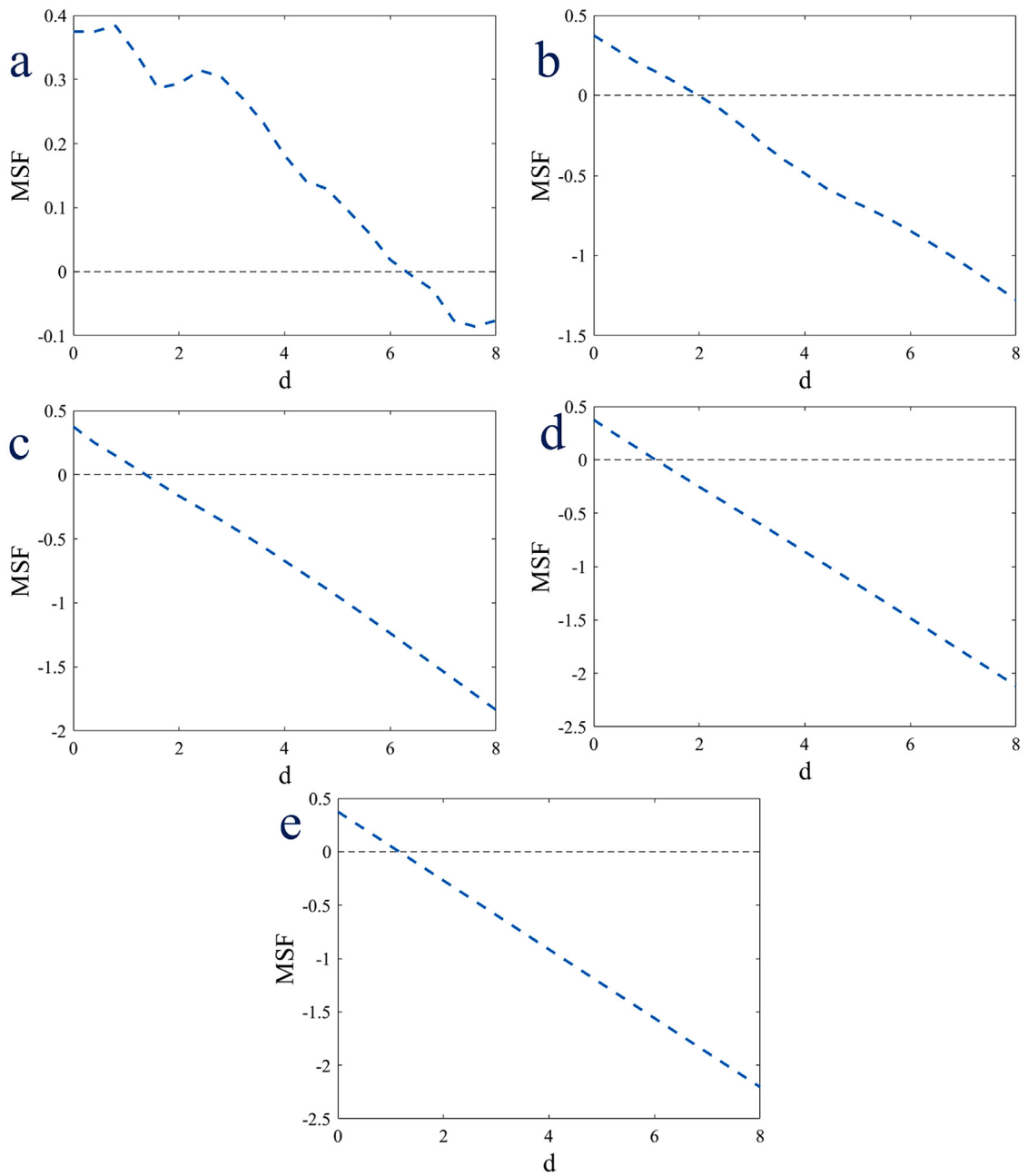


Fig. 4. The MSF of five cases for coupled piecewise linear oscillator; a) case 1-Table 1; b) case 2-Table 1; c) case 3-Table 1; d) case 4-Table 1; e) case 5-Table 1; The smallest zero crossings of the MSF function is in case 5 in which all variables are coupled equally with the same coupling coefficient 0.3333.

Table 1
Five different cases for the coupling structures in circulant oscillators.

Case1	$Vec_d = d * (1, 0, 0)^T$
Case2	$Vec_d = d * (0.6, 0.2, 0.2)^T$
Case3	$Vec_d = d * (0.4, 0.33, 0.27)^T$
Case4	$Vec_d = d * (0.3333, 0.3533, 0.3133)^T$
Case5	$Vec_d = d * (0.3333, 0.3333, 0.3333)^T$

Table 2
The optimum coupling strength of synchronization (zero crossing of MSF diagram) in different coupling cases for four circulant oscillators.

Zero Crossings	Case 1	Case 2	Case 3	Case 4	Case 5
	$\begin{bmatrix} 1 \\ 0 \\ 0 \end{bmatrix}$	$\begin{bmatrix} 0.6 \\ 0.2 \\ 0.2 \end{bmatrix}$	$\begin{bmatrix} 0.4 \\ 0.33 \\ 0.27 \end{bmatrix}$	$\begin{bmatrix} 0.3333 \\ 0.3533 \\ 0.3133 \end{bmatrix}$	$\begin{bmatrix} 0.3333 \\ 0.3333 \\ 0.3333 \end{bmatrix}$
Sys 1	$d = 6.301$	$d = 1.9826$	$d = 1.367$	$d = 1.1714$	$d = 1.1622$
Sys 2	$d = 0.4776$	$d = 0.4528$	$d = 0.4256$	$d = 0.4042$	$d = 0.3888$
Sys 3	$d = 0.6834$	$d = 0.4154$	$d = 0.3842$	$d = 0.377$	$d = 0.3172$
Sys 4	$d = 6.5146$	$d = 2.4432$	$d = 1.7862$	$d = 1.4874$	$d = 1.0564$

Table 3
Six different cases for coupling structures in the Lorenz oscillator.

Case1	$Vec_d = d * (1, 0, 0)^T$
Case2	$Vec_d = d * (0, 1, 0)^T$
Case3	$Vec_d = d * (0, 0, 1)^T$
Case4	$Vec_d = d * (0.3333, 0.3333, 0.3333)^T$
Case5	$Vec_d = d * (0.8, 0.1, 0.1)^T$
Case6	$Vec_d = d * (0.666, 0.193, 0.141)^T$

Table 4
The optimum coupling strength of synchronization (zero crossing of MSF diagram) in the six different coupling cases for Lorenz oscillator.

Zero Crossings	Case 1	Case 2	Case 3	Case 4	Case 5	Case 6
	$\begin{bmatrix} 1 \\ 0 \\ 0 \end{bmatrix}$	$\begin{bmatrix} 0 \\ 1 \\ 0 \end{bmatrix}$	$\begin{bmatrix} 0 \\ 0 \\ 1 \end{bmatrix}$	$\begin{bmatrix} 0.3333 \\ 0.3333 \\ 0.3333 \end{bmatrix}$	$\begin{bmatrix} 0.8 \\ 0.1 \\ 0.1 \end{bmatrix}$	$\begin{bmatrix} 0.666 \\ 0.193 \\ 0.141 \end{bmatrix}$
	$d = 7.61$	$d = 2.11$	$d = 1.7$	$d = 2.55$	$d = 4.23$	$d = 3.53$

Table 5
Seven different cases for coupling structures in the Rössler oscillator.

Case1	$Vec_d = d * (1, 0, 0)^T$
Case2	$Vec_d = d * (0, 1, 0)^T$
Case3	$Vec_d = d * (0, 0, 1)^T$
Case4	$Vec_d = d * (0.3333, 0.3333, 0.3333)^T$
Case5	$Vec_d = d * (0.5, 0.5, 0)^T$
Case6	$Vec_d = d * (0.6, 0.4, 0)^T$
Case7	$Vec_d = d * (0.9187, 0.0813, 0)^T$

coupling cases are defined related to the oscillator’s dynamics. Three cases are coupling of the x variable, coupling of the y variable, and coupling of the z variable. The fourth case is coupling through all variables equally. To define other meaningful cases, we consider the zero crossings of the MSF functions of the coupling for each variable. For example, if the zero-crossing in coupling through the z variable is smaller than through the y or x variable, this means that the z variable has a more powerful coupling effect on the synchronization of the two oscillators. Thus we define a coupling vector with coupling coefficients whose x part is a fraction of the zero crossing of the MSF on the x variable divided to the sum of zero crossings of the MSF function on each variable separately. The y and z parts of the coupling vector are calculated with the same structure as for the y and z variables. This case is called an exact proportion of zero-crossings. Some other coupling cases are defined randomly between these cases.

In the Lorenz oscillator, six coupling cases are defined, as shown in Table 3. The zero-crossings of the MSF function for each coupling case of the Lorenz oscillator are shown in Table 4. The results show that the smallest zero-crossing of the MSF is in case 3. This means that coupling the z variable is the most effective case. In this case, synchronization happened for the smallest coupling parameter compared with the other cases.

Seven cases are defined to test the Rössler oscillator’s synchronization parameter, which are shown in Table 5. The first four cases are the same as in the Lorenz oscillator. The seventh case is the exact proportion of zero-crossings. Cases 5 and 6 are randomly selected among the cases.

The zero-crossings of the MSF for each case are shown in Table 6. The results show the smallest synchronization parameter is in case 2.

The other studied oscillator is the HR neuron. Five coupling cases are studied in this oscillator (Table 7). Case 4 has the minimum coupling parameter for synchronization.

Table 6

The optimum coupling strength of synchronization (zero crossing of MSF diagram) in seven different coupling cases for Rössler oscillator.

	Case 1	Case 2	Case 3	Case 4	Case 5	Case 6	Case 7
	$\begin{bmatrix} 1 \\ 0 \\ 0 \end{bmatrix}$	$\begin{bmatrix} 0 \\ 1 \\ 0 \end{bmatrix}$	$\begin{bmatrix} 0 \\ 0 \\ 1 \end{bmatrix}$	$\begin{bmatrix} 0.3333 \\ 0.3333 \\ 0.3333 \end{bmatrix}$	$\begin{bmatrix} 0.5 \\ 0.5 \\ 0 \end{bmatrix}$	$\begin{bmatrix} 0.6 \\ 0.4 \\ 0 \end{bmatrix}$	$\begin{bmatrix} 0.9187 \\ 0.0813 \\ 0 \end{bmatrix}$
Zero Crossings	$d = 0.192$ $d = 4.62$	$d = 0.1691$	-	$d = 0.26$	$d = 0.1745$	$d = 0.18$	$d = 0.19$

Table 7

Five different cases for coupling structures in the HR oscillator.

Case1	$Vec_d = d * (1, 0, 0)^T$
Case2	$Vec_d = d * (0, 1, 0)^T$
Case3	$Vec_d = d * (0, 0, 1)^T$
Case4	$Vec_d = d * (0.3333, 0.3333, 0.3333)^T$
Case5	$Vec_d = d * (0.9091, 0.0909, 0)^T$

Table 8

The optimum coupling strength of synchronization (zero crossing of MSF diagram) in five different coupling cases for HR oscillator.

	Case 1	Case 2	Case 3	Case 4	Case 5
	$\begin{bmatrix} 1 \\ 0 \\ 0 \end{bmatrix}$	$\begin{bmatrix} 0 \\ 1 \\ 0 \end{bmatrix}$	$\begin{bmatrix} 0 \\ 0 \\ 1 \end{bmatrix}$	$\begin{bmatrix} 0.3333 \\ 0.3333 \\ 0.3333 \end{bmatrix}$	$\begin{bmatrix} 0.9091 \\ 0.0909 \\ 0 \end{bmatrix}$
Zero Crossings	$d = 0.848$	$d = 0.1728$	-	$d = 0.1199$	$d = 0.5831$

4. Conclusion

The effect of single-variable couplings, multi-variable couplings with equal coupling coefficients, and multi-variable couplings with non-equal coupling coefficients on synchronization was studied in this paper. The goal was to find the best coupling structure, which results in the minimum coupling parameter for synchronization. To compare the results of various coupling structures, the sum of all coupling parameters in all cases was considered to be equal. The coupled systems consist of two categories of oscillators studied in this paper: circulant oscillators, and non-circulant oscillators. The results show that in circulant oscillators, the best coupling structure with the smallest coupling parameter of synchronization was multi-variable coupling with equal coupling coefficients. However, in non-circulant oscillators, there is not such a result, since in various oscillators, the smallest coupling parameter does not belong to a specific coupling structure. For example, in Lorenz coupled oscillators, the optimum coupling structure is Case 3 (z coupling), while in Rössler coupled oscillators, the optimum coupling is Case 2 (y coupling).

Declaration of Competing Interest

The authors declare no conflict of interest.

Acknowledgment

This work was partially supported by Iran Science Elites Federation (Grant no. M-97171). Matjaž Perc was supported by the Slovenian Research Agency (Grant nos. P1-0403 and J1-2457).

References

- [1] U. Feudel, W. Jansen, J. Kurths, Tori and chaos in a nonlinear dynamo model for solar activity, *Int. J. Bifur. Chaos* 3 (1993) 131–138.
- [2] J.C. Sprott, Some simple chaotic flows, *Phys. Rev. E* 50 (1994). R647–R650
- [3] A. Calim, J.J. Torres, M. Ozer, M. Uzuntarla, 2020, Chimera states in hybrid coupled neuron populations, *Neural Netw.* 126, 108–117,
- [4] E. Tlelo-Cuautle, J. Rangel-Magdaleno, A. Pano-Azucena, P. Obeso-Rodelo, J.C. Nuñez Perez, FPGA realization of multi-scroll chaotic oscillators, *Commun. Nonlinear Sci. Numer. Simul.* 27 (2015) 66–80.
- [5] D. Peng, K. Sun, S. He, A.O. Alamodi, What is the lowest order of the fractional-order chaotic systems to behave chaotically? *Chaos Solitons Fract.* 119 (2019) 163–170.
- [6] J. Ruan, K. Sun, J. Mou, S. He, L. Zhang, Fractional-order simplest memristor-based chaotic circuit with new derivative, *Eur. Phys. J. Plus* 133 (2018) 1–12.
- [7] C. Li, G. Chen, Chaos in the fractional-order Chen system and its control, *Chaos Solitons Fract.* 22 (2004) 549–554.
- [8] C. Li, K. Su, L. Wu, Adaptive sliding mode control for synchronization of a fractional-order chaotic system, *J. Comput. Nonlinear Dyn.* 8 (2012) 031005.

- [9] P. Ramazza, S. Boccaletti, A. Giaquinta, E. Pampaloni, S. Soria, F. Arecchi, Pattern formation in a nonlinear optical system: the effects of nonlocality, *Chaos Solitons Fract.* 10 (1999) 693–700.
- [10] S. Boccaletti, W. Ditto, G. Mindlin, A. Atangana, Modeling and forecasting of epidemic spreading: the case of Covid-19 and beyond, *Chaos Solitons Fract.* 135 (2020) 109794.
- [11] Z. Wang, Y. Moreno, S. Boccaletti, M. Perc, Vaccination and epidemics in networked populations—an introduction, *Chaos Solitons Fract.* 103 (2017) 177–183.
- [12] A. Agarwal, N. Marwan, M. Rathinasamy, B. Merz, J. Kurths, Multi-scale event synchronization analysis for unravelling climate processes: a wavelet-based approach, *Nonlinear Processes Geophys.* 24 (2017) 599–611.
- [13] M. Uzuntarla, Firing dynamics in hybrid coupled populations of bistable neurons, *Neurocomputing* 367 (2019) 328–336.
- [14] A. Pikovsky, M. Rosenblum, J. Kurths, *Synchronization: a Universal Concept in Nonlinear Sciences*, Cambridge university press, 2003.
- [15] M. Uzuntarla, J.J. Torres, A. Calim, E. Barreto, Synchronization-induced spike termination in networks of bistable neurons, *Neural Netw.* 110 (2019) 131–140.
- [16] S. Boccaletti, J. Kurths, G. Osipov, D. Valladares, C. Zhou, The synchronization of chaotic systems, *Phys. Rep.* 366 (2002) 1–101.
- [17] A. Calim, P. Hövel, M. Ozer, M. Uzuntarla, Chimera states in networks of type-I Morris-Lecar neurons, *Phys. Rev. E* 98 (2018) 062217.
- [18] A. Stefanski, T. Kapitaniak, Using chaos synchronization to estimate the largest Lyapunov exponent of nonsmooth systems, *Discret. Dyn. Nat. Soc.* 4 (2000) 968905.
- [19] F. Nazarimehr, S. Panahi, M. Jalili, M. Perc, S. Jafari, B. Ferčec, Multivariable coupling and synchronization in complex networks, *Appl. Math. Comput.* 372 (2020) 124996.
- [20] X. Zhang, F. Wu, J. Ma, A. Hobiny, F. Alzahrani, G. Ren, Field coupling synchronization between chaotic circuits via a memristor, *AEU Int. J. Electron. Commun.*, 2020, 115, 153050.
- [21] S. He, K. Sun, H. Wang, Dynamics and synchronization of conformable fractional-order hyperchaotic systems using the homotopy analysis method, *Commun. Nonlinear Sci. Numer. Simul.* 73 (2019) 146–164.
- [22] S. Majhi, D. Ghosh, J. Kurths, Emergence of synchronization in multiplex networks of mobile Rössler oscillators, *Phys. Rev. E* 99 (2019) 012308.
- [23] S. Mostaghimi, F. Nazarimehr, S. Jafari, J. Ma, Chemical and electrical synapse-modulated dynamical properties of coupled neurons under magnetic flow, *Appl. Math. Comput.* 348 (2019) 42–56.
- [24] M. Ge, L. Lu, Y. Xu, X. Zhan, L. Yang, Y. Jia, Effects of electromagnetic induction on signal propagation and synchronization in multilayer Hindmarsh-Rose neural networks, *Eur. Phys. J. Spec. Top.* 228 (2019) 2455–2464.
- [25] C.W. Wu, L.O. Chua, Synchronization in an array of linearly coupled dynamical systems, *IEEE Trans. Circ. Syst. I Fundam. Theory Appl.* 42 (1995) 430–447.
- [26] L.M. Pecora, T.L. Carroll, Master stability functions for synchronized coupled systems, *Phys. Rev. Lett.* 80 (1998) 2109–2112.
- [27] S.N. Chowdhury, S. Majhi, M. Ozer, D. Ghosh, M. Perc, Synchronization to extreme events in moving agents, *New J. Phys* 21 (2019) 073048.
- [28] C.I. del Genio, J. Gómez-Gardeñes, I. Bonamassa, S. Boccaletti, Synchronization in networks with multiple interaction layers, *Sci. Adv.* 2 (2016), E1601679
- [29] J. Zhao, D.J. Hill, T. Liu, Synchronization of dynamical networks with nonidentical nodes: criteria and control, *IEEE Trans. Circ. Syst. I Regul. Pap.* 58 (2011) 584–594.
- [30] G. Gugapriya, K. Rajagopal, A. Karthikeyan, B. Lakshmi, A family of conservative chaotic systems with cyclic symmetry, *Pramana* 92 (2019) 48.
- [31] K. Rajagopal, A. Akgul, V.-T. Pham, F.E. Alsaadi, F. Nazarimehr, F.E. Alsaadi, S. Jafari, Multistability and coexisting attractors in a new circulant chaotic system, *Int. J. Bifur. Chaos* 29 (2019) 1950174.
- [32] J.C. Sprott, *Elegant Chaos: Algebraically Simple Chaotic Flows*, World Scientific, 2010.
- [33] L. Huang, Q. Chen, Y.-C. Lai, L.M. Pecora, Generic behavior of master stability functions in coupled nonlinear dynamical systems, *Phys. Rev. E* 80 (2009) 036204.